Phenomenology and system engineering of micro- and nano-antenna FPA sensors for detection of concealed weapons and improvised explosive devices

R. Appleby* and S. Ferguson
The Institute of Electronics, Communications and Information Technology (ECIT), Queen's University Belfast, NI Science Park, Queen's Road, Queen's Island, Belfast, Northern Ireland, BT3 9DT.

ABSTRACT

The ability of millimetre wave and terahertz systems to penetrate clothing is well known. The fact that the transmission of clothing and the reflectivity of the body vary as a function of frequency is less so. Several instruments have now been developed to exploit this capability. The choice of operating frequency, however, has often been associated with the maturity and the cost of the enabling technology rather than a sound systems engineering approach. Top level user and systems requirements have been derived to inform the development of design concepts. Emerging micro and nano technology concepts have been reviewed and we have demonstrated how these can be evaluated against these requirements by simulation using OpenFx. Openfx is an open source suite of 3D tools for modeling, animation and visualization which has been modified for use at millimeter waves.

Keywords: Millimetre wave, Terahertz, Concealed weapons, nano-antenna, micro antenna, simulation, modeling.

1. INTRODUCTION

The millimetre wave part of the spectrum which sits between the visible and microwave regions has the advantage that it can be used to penetrate clothing and is ideal for the detection of concealed weapons and improvised explosive devices. Systems have been designed to screen people as they enter a secure area and are now deployed in airports and many other facilities. Two types have been developed, passive systems which image the natural radiation reflected and emitted by objects in the scene and active systems which have a transmitter and irradiate the scene, and then image the reflected signal. Both types are widely deployed and examples include the active Provision System from L3[1] and a passive system from Microsemi (Brijot)[2].

To date, the systems that have been developed draw heavily on technology from the microwave region using waveguide techniques to collect the radiation and solid state receivers to amplify and detect it before image processing for display. The number of receivers has been limited due to their cost and the fact that they have relatively high sensitivity and can therefore be used in systems which are scanned. In the receivers of these systems when the radiation transitions from free space to a guided medium and then to a solid state device there is usually some form of micro or nano engineering. For instance, the transition from waveguide to microstrip at 94GHz requires a probe[3] with dimensions of order of 100μm. The active devices typically use lithography and structures which are ~0.1μm in size. Focal Plane Array (FPA) technology similar to that typically found in infrared or visible camera has not been developed although some research has been reported.

The ability to fabricate nano and micro antennas has recently given rise to research were devices which are significantly smaller than the operating wavelength are used to manipulate electromagnetic radiation. Nano antennas have found recent application in coupling infrared and visible light into semiconductor devices or other structures. Typical examples include solar cells, colour filters and many other applications. Micro antennas have been reported at 43GHz[4] with an adaptive microstrip patch antenna using a MEMS device. Patch antennas are not normally used in imaging due to their relatively high loss.

* r.appleby@qub.ac.uk

Micro- and Nanotechnology Sensors, Systems, and Applications IV, edited by Thomas George, M. Saif Islam, Achyut Dutta, Proc. of SPIE Vol. 8373, 837329
 · doi: 10.1117/12.918826

In Section 2 we outline the basic principles of systems engineering and how they can be applied to millimeter wave camera design concepts for the detection of concealed weapons and improvised explosive devices. This paper mainly discusses passive imaging but references to active imaging will be made were appropriate to highlight the differences. Section 3 defines the key parameters associated with system performance and section 4 the phenomenology or optical properties of the targets and backgrounds at millimeter waves. Section 5 summarises the current state of the art in FPA technology and section 6 discusses how simulation can be used in systems engineering to evaluate different design concepts.

2. SYSTEMS ENGINEERING

The term "Systems Engineering" can be traced back[5] to the Bell telephone Laboratories in the 1940s[6]. The need to identify and manipulate the properties of a system as a whole, which in complex engineering projects may greatly differ from the sum of the parts' properties, was recognised[7]. System engineering is a robust approach to the design, creation, and operation of systems. In simple terms, the approach consists of identification and quantification of system goals, creation of alternative system design concepts, performance of design trades, selection and implementation of the best design, verification that the design is properly built and integrated, and post-implementation assessment of how well the system meets (or met) the goals[8]. It also encourages the use of modeling and simulation to validate assumptions or theories on systems and the interactions within them[9,10].

As shown in

Figure **1**, this can be expressed in a simple diagram where the need for a new capability is expressed in a User Requirement Document (URD) which in turn leads to a Systems Requirement Document (SRD) that express the URD in technical language. Against the SRD new concepts are generated, some of which will eventually lead to equipment designs. Throughout this process the user requirements expressed in the URD are paramount in guiding the project and it is this which ultimately leads to the successful operation of the system.

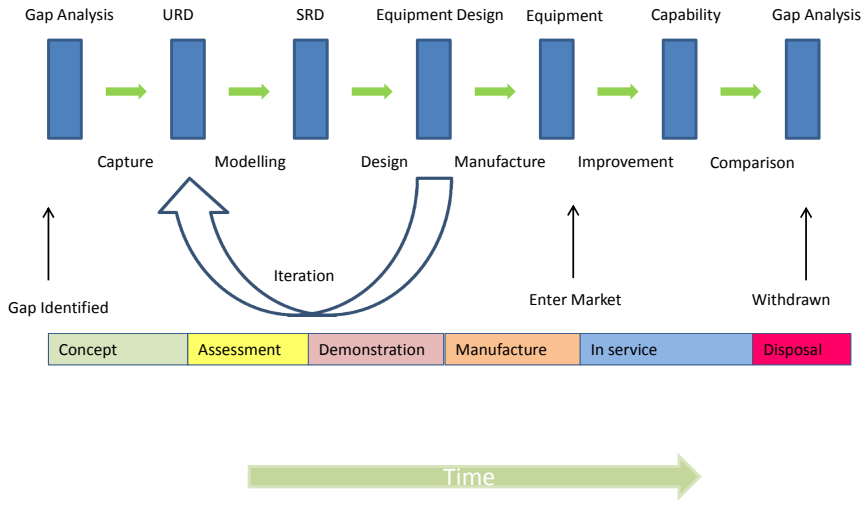

Figure 1 Systems Engineering process

Whilst System Engineering is clearly relevant to large multi-disciplinary projects such as a space craft, its relevance to research on new technology might be questioned. However if one defines the system as comprising of everything from the scene being imaged to the observer, as shown in Figure 2, one can see the relevance. Just because the system uses a brand new widget it does not necessarily mean it will be improved!

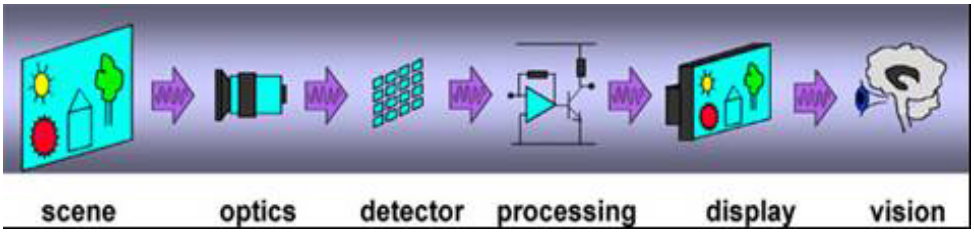

Figure 2 Imaging System

The Systems Engineering discipline ensures that the equipment concept being offered is fit for purpose. Whilst it is beyond the scope of this paper to formally adopt a Systems Engineering process we will consider the first three steps in Figure **1** i.e. URD, SRD and Equipment Design. We will show how simulation can be used to evaluate concepts which are emerging from micro and nano antennas.

2.1 User Requirements Document

There are three different requirements which drive systems design for concealed weapons and improvised explosive device detection. The first is a portal deployed at a security check point where the person is cooperative; the second a stand-off system to monitor people at a distance of tens of meters and the third which is a walk through portal where the range is a few meters. In all cases the target set given in Table 1 is similar and there is a requirement to perform detection and recognition through clothing whilst maintaining a person's privacy.

Table 1 Target set

Object	**Material**
Gun	Metal
Knife	Metal/Ceramic
Explosive	Explosives
Improvised explosive device	Explosive with shrapnel
Body	Skin
Clothing	Cotton/Synthetic fabrics

Further details of the millimetre wave properties of these materials are provided in Section 4.

2.2 Systems Requirement Document

The primary requirements are listed in Table 2 with the assumption that a 20mm spot size and a thermal sensitivity of <1K are sufficient to meet user needs[11]. There are other secondary requirements such as size, weight and power which are also important but are not discussed here.

2.3 Portal

Here a subject is scanned at a range of <1 m and the subject enters and either rotates, or the equipment rotates around them, facilitating a 360 degree scan. The subject being scanned cooperates with the instructions provided by the operator. This type of instrument is normally a fixed installation. The key parameters are listed in Table 2. The field of view is such that it will cover a person at 1m range.

2.4 Stand-off

In this scenario a subject is scanned at a range of greater than 10m and is non-cooperative. The subject is entering an area of interest and being monitored by the system. Longer ranges are of greater interest so that the operator and equipment can be at a safe distance from the threat. Two systems may be required, one to observe the back and the other to observe

the front of a subject. It is also possible to use infrastructure to cause the subject to present both sides; for example passing through a barrier or check point could allow this. The key parameters are listed in Table 2 for operation at 20 m.

Table 2 System parameters for security imaging

Parameter	Portal	Stand-off >10m	Walkthrough
Range	<1 m	20 m	>3m
Field of View (v x h degrees)	90 x 45	2 x 5	40 x 20
Frame time (s)	1-2	<0.1	<0.1
Angular resolution (mrad)	20	1	7
Thermal Sensitivity (K)	<1	<1	<1

2.5 Walk through

In this scenario a subject is passing through an area where they will be screened but they are free to move through it. There is a need to be able to scan both sides of a person and monitor them from when they enter until they leave the area. This is an emerging requirement for next generation airport security systems to improve the passenger experience[12].

The three requirements listed in Table 2 demand very different systems solutions and would probably give rise to three separate URDs. The key system parameters required to achieve the performance listed in Table 2 are discussed in the following section.

3. SYSTEM PERFORMANCE

A system is needed which is able to detect the temperature differences in the scene described in Section 4 and see the small features present in some objects. System Performance is a complex issue which involves many trade-offs and has been previously reviewed[11,13]. Here we will only concern ourselves with spatial resolution, thermal sensitivity, sampling and field of view.

3.1 Spatial Resolution

The spatial resolution (or beamwidth) of the imager is governed by the point spread function of the optics (or antenna). This resolution is equal to the full width at half power of the point spread function. For high quality (diffraction-limited) optics, the angular resolution θ of the sensor will be given by the Rayleigh formula:

$$\sin\theta = \frac{1.22\lambda}{D} \tag{1}$$

where λ is the wavelength and D is the effective aperture of the optics

3.2 Thermal sensitivity

For a simple total-power radiometer imaging system where the receiver is always looking at an extended object, the thermal sensitivity of the receiver is given by the ideal radiometer equation

$$\Delta T = \frac{T_A + T_S}{\sqrt{\beta\tau}} \tag{2}$$

where T_A is the noise temperature of the antenna, T_S is the receiver noise temperature (the double-sideband value if the receiver is a superheterodyne), β is the bandwidth (RF bandwidth for a direct detection or IF bandwidth for a superheterodyne receiver) and τ is the integration time. This equation assumes that the only form of noise is thermal noise. Additional forms of noise can reduce sensitivity.

3.3 Low Frequency noise

In practice, receivers also suffer from 1/f noise, typically caused by gain fluctuations, leading to a more realistic radiometer equation:

$$\Delta T = \left(T_A + T_S\right)\sqrt{\frac{1}{\beta\tau} + \left(\frac{\Delta G}{G}\right)^2} \qquad (3)$$

where G is the gain and ΔG are the RMS fluctuations associated with this gain. Since these gain fluctuations vary approximately as 1/(post-detection frequency), increasing the integration time will increase the noise, due to these gain fluctuations, at the same time as reducing the white noise. Therefore, thermal sensitivity will not increase without limit as integration times become longer.

Slow variations in the gain of a receiver can give rise to non-uniformity in the image with artifacts such as scan lines appearing. These can limit the performance of the system particularly if fine features need to be observed.

3.4 Sampling

In order for all the detail resolved by the optics to be captured by the receivers and presented as an image to an operator, the image must be adequately sampled. The criterion normally applied is the Nyquist criterion, namely that in each direction there should be two samples per beamwidth (as given by the Rayleigh formula). Sampling rates significantly lower than this lose detail. Note, however, that sampling rates higher than this do not significantly increase detail, but either reduce the SNR or require more receivers (thus increasing complexity, power requirements and cost).

Clearly, if the sampling rate is less than half-Nyquist (one pixel per beamwidth) then this will directly affect the size of targets that may be discriminated. Furthermore, as Figure 3 below makes clear, sampling at half-Nyquist can also substantially affect the capability of the system to resolve narrow targets:

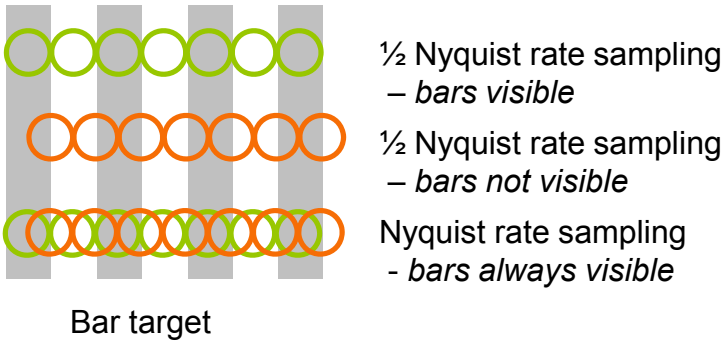

Figure 3 The effect of sampling rates on just-resolved bar target (Bar target =sensor beamwidth)

Sampling at the Nyquist rate is therefore preferred. Good sampling is achieved by close packing the receivers and their associated antennas but care must be taken in design to minimize spillover[14] where the receiver will pick up radiation from outside the primary aperture.

3.5 Field of View

The instantaneous field of view of imaging systems typically used in security scanning is an important parameter particularly at short range where a subject can subtend a large angle (90°). The off axis performance of lenses and mirrors is therefore important. Chromatic aberrations do not constrain the optical design as they might in the visible or infrared as the materials used tend to have a refractive index which does not vary significantly. Field curvature can often be dealt with by curving the receiver array. Distortion may be corrected by scan conversion algorithms in the back end processing. It is spherical aberration, astigmatism and coma which restrict performance.

Smith[15] describes the application of various lens and mirror optical designs in the visible and IR in terms of aperture and field of view. Much of this also applies to millimetre wave imagers. However, the fields of view possible with a given aperture are increased because of the generally lower angular resolution and by only having to correct spherical aberration, coma and astigmatism. It is clear that to meet the requirement for a wide field of view with fast optics either a complex multi-lens arrangement will be required, or a multiple mirror/catadioptic system.

System performance will also be influenced by the optical properties of the weapons and devices and these are discussed in the next section.

4. PHENOMENOLOGY

An object is visible to an imaging system when its temperature difference from the background exceeds the signal to noise ratio of that system. The temperature difference (ΔT_{diff}) is defined as:

$$\Delta T_{diff} = T_T - T_B \tag{4}$$

where T_T is the radiometric temperature of the target or object we are observing and T_B is the radiometric temperature of the background. The radiometric temperature is the temperature of a black body that would provide the same signal and is not the physical temperature of the object.

The radiometric temperature of an object is a function of its optical properties i.e. emissivity *(ε)*, reflectivity *(r)*and transmission *(t)* in the waveband of interest and is given by:

$$T_T = rT_e + \varepsilon T + tT_B \tag{5}$$

where T_e is the radiometric temperature of the environment reflected from the object so outdoors this would be the sky temperature or indoors the rooms radiometric temperature and T is the physical temperature of the object. It should be noted that:

$$\varepsilon + r + t = 1 \tag{6}$$

In the millimetre and sub millimetre wave part of the spectrum emissivity, transmission and reflectivity have been previously reported[13] up to frequencies of 1THz and are reproduced in Table 3. In this frequency band the spectra of most solid materials are almost frequency independent as vibrational spectra typical occur at higher frequencies[16]. The exceptions to this are items which contain water or those with particles or structures that are similar in size to the wavelength when scattering can become a mechanism for increasing loss. This type of scattering can easily be mistaken for absorption.

Table 3 Optical properties of 5 mm thick explosives, skin, metal, denim and t-shirt[13]

	Emissivity (*ε*)			**Reflectivity (*r*)**			**Transmission (*t*)**		
	100 GHz	500 GHz	1 THz	100 GHz	500 GHz	1 THz	100 GHz	500 GHz	1 THz
Explosive on skin	0.76	0.95	0.94	0.24	0.05	0.06	0	0	0
Metal	0	0	0	1	1	1	0	0	0
Skin	0.65	0.91	0.93	0.35	0.09	0.07	0	0	0
Denim	0.09	0.49	0.85	0.01	0.01	0.05	0.9	0.5	0.1
tee-shirt	0.04	0.2	0.3	0	0	0.05	0.96	0.8	0.65

The optical properties of skin are dominated by its water content, it has a reflectivity of 0.35 at 100GHz but this reduces to 0.07 at 1THz. As the reflectivity decreases, the emissivity increases from 0.65 to 0.93 respectively. Most clothing is transparent and metals are highly reflecting. Explosives on skin also show a decrease in reflectivity with increase in frequency which is caused by scattering[17].

A simple model of the thermal contrast can be constructed with a set of simultaneous equations[18,19] and it can be shown that indoors, with an environmental temperature of 300K, the temperature difference between metal and the body and explosives and the body is of the order of 5K. It should be noted that this contrast will increase significantly if the imaging system is operating outdoors or the scene is illuminated with a man-made source.

5. FOCAL PLANE ARRAY TECHNOLOGY

FPAs are now common place in infrared and visible camera but to date have not been developed for millimetre wave systems. There has, however, been some research and in the microwave region and the integration of IF amplifiers onto crossed diploes operating at X Band [20] was reported. Rutledge [21] reported a monolithic two dimensional horn imaging array operating at 93 and 242GHz using 4 μm square micro-bolometers mounted at the centre of a dipole and whilst this demonstrated the principle of integration it lacked sensitivity for security imaging.

Two approaches have provided the necessary thermal sensitivity and some examples are discussed below. The first uses gain either at IF in a heterodyne receiver or at RF in a direct detection receiver and the second uses a bolometer cooled to low temperature. Figure 4 shows a 64 element array of 94GHz direct detection receivers[22,23], using indium phosphide monolithic microwave integrated circuits to provide ~50dbs of gain before a gallium arsenide Schottky detector. There are eight modules each with eight receivers and the horns from each are close packed and can be seen in a curved focal plane. Each receiver is individually packaged in metal due to the high gain required to overcome the noise floor of the detector.

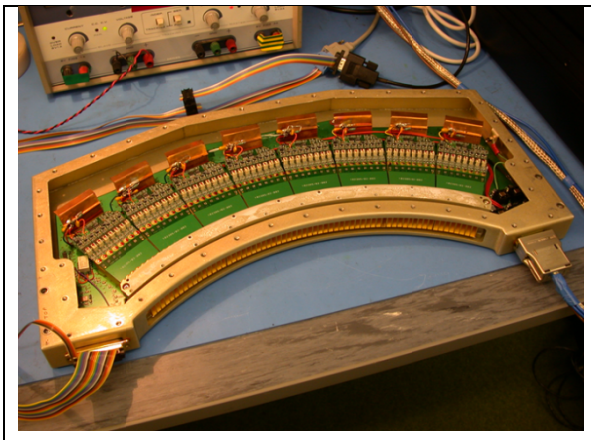

Figure 4 94GHz FPA using 64 Direct Detection Receivers[22] (Cover removed)

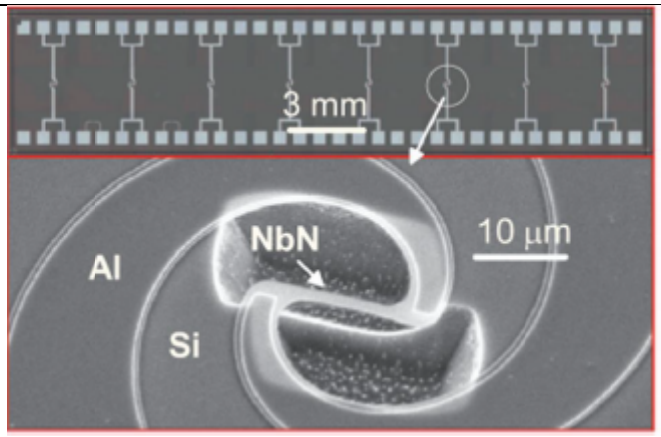

Figure 5 NbN Superconducting antenna coupled hot spot microbolometer[24]

By replacing the gallium arsenide diode with a Sb-heterostructure backward tunnel diode detector [25] the gain can be reduced to 25dbs. The chipset in this case is ~5mm long and 1mm wide but still requires packaging to isolate the amplifier detector and associated bias circuits from electromagnetic interference.

Figure 5 shows a single Niobium Nitride (NbN) which is a superconducting bolometer[24] and has been used to build array of up to 128 elements but does require cryogenic cooling. Here the bolometer is of the order of 10 μm in size and the spiral antenna is used to couple extremely wide bandwidth radiation (0.2 -1THz) into the device.

A wafer scale integrated FPA utilising semiconductor devices was proposed by Asley[26] operating at 200GHz and utilising indium antimonide technology. It was proposed that every pixel of the two dimensional FPA had its own horn antenna, amplifier and detector which were readout through a hybridized silicon multiplexer as shown in Figure 6. An innovative part of this design was allowing the radiation to couple into MMIC through a hole in the ground plane which provided electrical isolation.

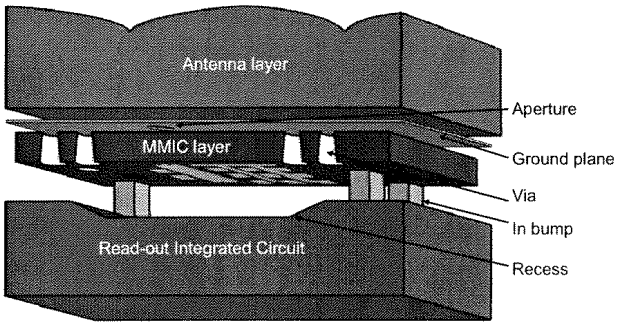

Figure 6 Schematic diagram of one pixel of the integrated array[26]

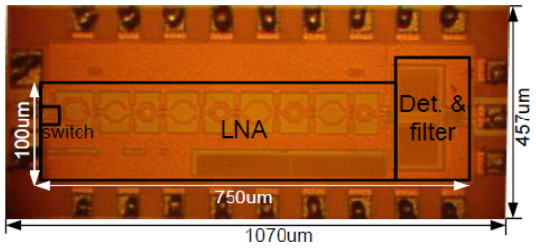

Figure 7 Dicke switched direct detection 94GHz receiver on CMOS[27]

There has recently been increased ineterest in using CMOS devices[27] as shown in Figure 7. This device which is ~ 1 x 0.5mm and contains an amplifier, detector and a Dicke switch. The performance of this device has recently been compared with one fabriacted in silicon germanium technology[28] and these results are shown in Table 4 which also compares the performance for all the detector technologies discussed here.

Table 4 Comparison for different detector technologies (*estimated value)

	Technology					
	0.12 µm SiGe[28]	65nm CMOS[27]	0.1µm InP[22,23,26]	InP[25]	In Sb[26]	NbN[24]
Atchitecture	Single ended	Differential	Single ended	Single ended	Single ended	Bolometer
NEP (fW/√Hz)	21	39				8
Responsivity (mV/W)	2.5~5	1.15				
NETD with 30ms integration time (K)	0.83	1.94	0.057	0.145	0.03*	0.007
Bandwidth(GHz)	80-110	99-111	75-99	75-102	220±20	200-1000
Power (mW)	35	57	200			

From this table it is clear that the InP, InSb and cooled NbN technologies have an NETD which is approximately an order of magnitude better than CMOS or SiGe for a 30ms integration time. Arrays of lens coupled detectors in CMOS and SOI technology have been used in active imagery at 600[29] and 825GHz[30]. An NEP of 17pw/√Hz was reported at 600GHz which will increase with frequency.

6. SIMULATION OF IMAGING CONCEPTS

Simulation can be used to evaluate the design concepts which use the different FPA array technologies described in section 5 against the top level requirements described earlier. For this purpose we have modified OpenFx[31] which is an open source suite of 3D tools for modeling animation and visualisation. The software consists of three main executable programs encapsulated in a container that hides this modularity from the user.

The software for the rendering module is compact and relatively short and thus it can be easily modified. The rendering module can operate quite independently of the modeling and animation modules. In this 'standalone' mode a 'script file' describes the scene and lists the objects that are to be visualized. Each object is defined in a separate file as a list of triangular polygons that represent its geometry, and its material properties, such as transparency and reflectivity. At the core of the renderer code is a surface illumination model. The illumination model takes into account diffuse, ambient and specular lighting and how this interacts with the surface material properties. A recursive ray-tracing algorithm follows on from a Z-buffer hidden surface stage allowing refraction, reflection and transparency to be simulated. In addition to this illumination model the software has a post processing stage where external modules can introduce effects such as motion blur, depth of field, camera lens aberrations, noise or any other image processing required.

For the simulation of millimeter wave systems two modifications were made to the renderer code as follows:

1. The illumination model (this is done on a per pixel basis) is replaced with an appropriate model for emission, reflection and transmission.
2. A post processing function is added to model the operation of a millimetre wave camera. This includes a noise generator, an averaging kernel to calculate the correct spatial resolution and scan patterns for scanned systems.

The simulation progresses in a manner analogous to the normal (optical) rendering in CGI. An output raster is defined; objects and other scene description items are loaded. A Z-buffer algorithm determines which object and polygon (or background) is visible in each raster pixel position. The illumination (and emission) model is then applied. Once each pixel in the raster has been rendered, the postprocessor phase passes a set of detectors across the image to determine the simulated millimeter wave output. This is then averaged and presented as the final image.

Figure 8 shows two images, one at 100GHz and the other at 500GHz, of a scene consisting of a clothed man inside a room with explosives on his chest and a knife on his right hip. The room is at a radiometric temperature of 300K and the images are produced without camera models.

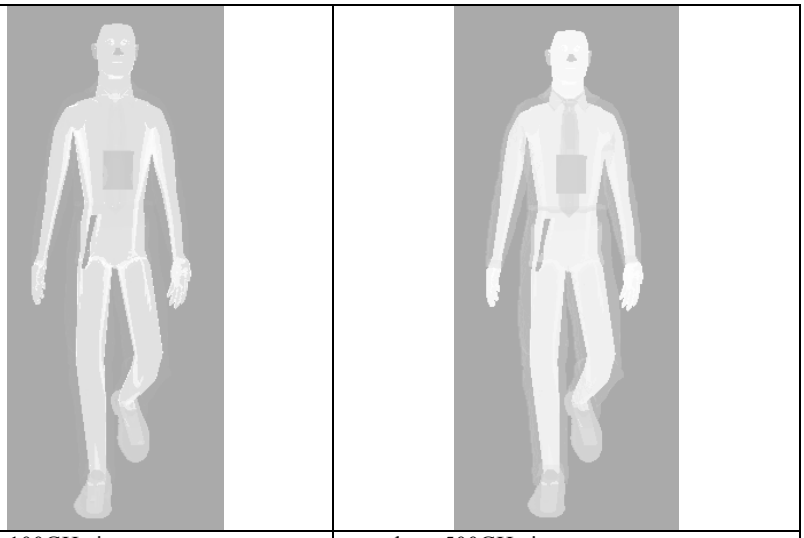

a. 100GHz image b. 500GHz image

Figure 8 Explosives on front torso and knife on right hip under light clothing

The optical properties of the materials are as described in Table 3 and the physical temperatures were 310K for skin and any object in contact with the body, the ears and nose were 305K and for an object close to the body, but not in contact, 305K. In the areas of the collar and tie the material transmission was reduced to account for the double thickness of cloth. The figure shows clearly that the body is more reflective at 100GHz with reflections of other body parts being visible and the slightly lower radiometric temperature.

The camera models listed in

Table 5 utilised the detector technologies (InP, NbN, 65nm CMOS) described in

Table 4 and were evaluated against the two scenes shown in Figure 8 with the results shown in Figure 9. In all cases an optical transmission of 0.5 is assumed. It should be noted that these are simulations only and do not represent real camera.

Table 5 Camera Models

Camera type	Frequency(GHz)	Detector Technology	Aperture(m)	Field of View (h x v degs)	No of Detectors
Linescan	94	InP	0.5	40 x 40	90
Conical Scan	600	NbN(cooled)	0.25	40 x 20	128
Starring array	99	65nmCMOS	0.5	25 x 25	65 x 65

If we assume the F number for the CMOS camera is 1 we have to reduce the field of view to ensure that the focal plane can be manufactured in a single wafer which in this case is assumed to be nine inches.

The camera model for the NbN receiver is over simplified as the material properties at 500GHz are used and the diffraction limited beamwidth is calculated at 600GHz. This detector has a bandwidth from 0.2 to 1THz and the material properties and the optical performance need to be modified to reflect this in future models. One approach would be to develop models for three separate cameras operating at say 0.2-0.4, 0.4-0.8 and 0.8-1THz and combine the results after simulation.

These images demonstrate that simulation of this nature can be used to evaluate different design concepts. It is clear from this simulation that camera systems based on 65nm CMOS cannot be used indoors without additional illumination and that systems operating at higher frequencies are more likely to be able to detect explosives.

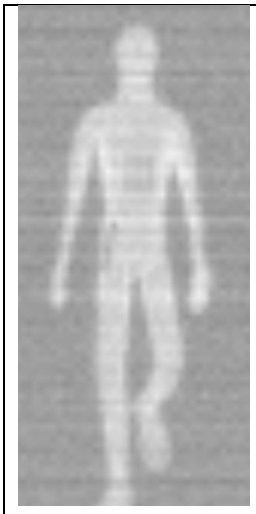

a. Linescan 94GHz InP

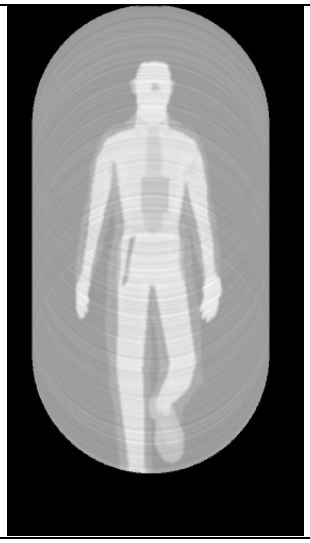

b. Conical scan 500GHz NbN

c. Starring array 99GHz 65nm CMOS

Figure 9 Simulated camera systems

a. Filename = man_100_turn.wmv http://dx.doi.org/10.1117/12.918826.1
b. Filename = man_500_turn.wmv http://dx.doi.org/10.1117/12.918826.2

7. CONCLUSIONS

The phenomenology associated with security imaging in the millimetre and sub-millimetre wave regions of the spectrum has been described. The current state of the art in integrated focal plane array technology, including indium phosphide, silicon CMOS, silicon germanium and niobium nitride bolometers, has been reviewed and it is clear that silicon receivers have lower thermal sensitivity. They could however find application in systems where active illumination is used.

The Systems Engineering approach has been used to outline top level user and associated system requirements. A simulation tool based on OpenFx has been developed and has been used to simulate camera system performance. This tool can be used to demonstrate that design concepts have adequate performance before starting detailed design and fabrication.

REFERENCES

[1] "Advanced Imaging Technology," ,http://www.sds.l-3com.com/products/advancedimagingtech.htm, Last accessed 22 Mar. 2012.

[2] "Gen 2," http://www.brijot.com/products/gen , Last accessed 22 Mar. 2012.

[3] Donadio, O., Elgaid, K., and Appleby, R., "Waveguide-to-microstrip transition at G-band using elevated E-plane probe," Electronics Letters, 47(2), 115-116 (2011).

[4] Haridas N., Erdogan A. T., Arslan T., and Begbie M., "Adaptive Micro-Antenna on Silicon Substrate," *First NASA/ESA Conference on Adaptive Hardware and Systems* (2006).

[5] "Systems engineering," http://en.wikipedia.org/wiki/Systems_engineering#cite_note-1, Last accessed 1 Mar. 2012.

[6] Schlager, J., "Systems engineering: key to modern development," IRE Transactions, 3(3), 64-66 (1956).

[7] Hall, A. D., A Methodology for Systems Engineering, Van Nostrand Reinhold, (1962).

[8] "NASA Systems Engineering Handbook," NASA,SP-610S, (1995).

[9] Smith, E. C., "Simulation in systems engineering," IBM Systems Journal, 1(1), 33-50 (1962).

[10] Sage, A. P. and Olson, S. R., "Modeling and Simulation in Systems Engineering," Simulation, 76(2), 90 (2001).

[11] Appleby R. and Anderton R. N., "Antennas and Security," *European Conference on Antennas and Propagation,* 1-6 (2007).

[12] "Study on the Competitiveness of the EU security industry," ECORYS, Rotterdam, The Netherlands, ENTR/06/054, (2009).

[13] Appleby, R. and Wallace, H. B., "Standoff detection of weapons and contraband in the 100 GHz to 1 THz region," IEEE Transactions on Antennas and Propagation, 55(11), 2944-2956 (2007).

[14] Anderton R. N., Appleby R., and Coward P. R., "Sampling passive millimetre wave imagery," *Proceedings of SPIE* 5989, 598915-10 (2005).

[15] Smith, W. J., "Automatic Lens design: Managing the Lens Design Program," in Modern Lens Design A Resource Manual. Eds.Fischer, R. E. and Smith, W. J. McGraw-Hill, 20, (1992).

[16] Appleby, R., "Passive millimetre-wave imaging and how it differs from terahertz imaging," Philosophical. Transactions of the Royal. Society London, Series. A, 362(1815), 379-394 (2004).

[17] Ortolani, M., Lee, J., Schade, U., and Huebers, H., "Surface roughness effects on the terahertz reflectance of pure explosive materials," Applied Physics Letters, 93(8) (2008).

[18] Appleby, R., Coward, P. R., and Sinclair, G. N., "Terahertz detection of illegal objects,". Eds.Miles, R. E., Zhang, X. C., Eisele, H., and Krotkus, A. Springer, 225-240, (2007).

[19] Appleby R. and Anderton R. N., "Imaging and sensing from 100 GHz to 1THz," 2009 Loughborough Antennas Propagation Conference (LAPC), 84-88 (2009).

[20] Alder, C. J., Brewitt-Taylor, C. R., Dixon, M., Hodges, R. D., Irving, L. D., and Rees, H. D., "Microwave and millimetre-wave receivers with integral antenna," IEE. Proceedings H., 138(3), 253-257 (1991).

[21] Rebeiz, G. M., Kasilingam, D. P., Guo, Y., Stimson, P. A., and Rutledge, D. B., "Monolithic millimeter-wave two-dimensional horn imaging arrays," IEEE Transactions on Antennas and Propagation, 38(9), 1473-1482 (1990).

[22] Anderton R. N., Appleby R., Beale J. E., Coward P. R., and Price S., "Security Scanning at 94GHz," *Proceedings of SPIE* 6211, 62110C-1-62110C-7 (2006).

[23] Humphreys R. G., Taylor S. M., Manning P. A., Munday P. D., and Powell J., "Performance of 94GHz receivers for passive imaging," *Proceedings of SPIE* 6548, 65480H-654810 (2007).

[24] Luukanen, A. and Pekola, J. P., "A superconducting antenna-coupled hot-spot microbolometer," Applied Physics Letters, 82(22), 3970-3972 (2003).

[25] Lynch, J. J., Harris, P. M., Schaffnewr, J. H., Royter, Y., Sokolich, M., Hughes, B., Schulman, J. N., and Yoon, Y. J., "Passive Millimeter-Wave Imaging Module with Preamplified Zero-Bias Detection," IEEE Transactions on Microwave Theory and Techniques, 56(7), 1592-1600 (2008).

[26] Ashley T., Adamson K. L., Ball G. J., Buckle P. D., Hall D. J., Lees D. J., Humphreys R. G., and Tang A. D., "Prospects for Integrated passive Millimetre Wave Focal Plane Arrays," *5th International EMRS DTC technical Conference* A16 (2008).

[27] Gu Q., Xu Z., Jian H.-Y., and Chang M.-C. F., "A CMOS Fully Differential W-Band Passive Imager with <2 K NETD ," RTU1C-2 , (2012).

[28] May, J. W. and Rebeiz, G. M., "Design and Characterization of W-Band SiGe RFICs for Passive Millimeter-Wave Imaging," IEEE Transactions on Microwave Theory and Techniques, 58(5) (2010).
[29] Sherry H., Hadil R. A., Grzyb J., Ojefors E., Cathelin A., Keiser A., and Pfeiffer U. R., "Lens-Integrated THz Imaging Arrays in 65nm CMOS Technologies," *IEEE RFIC* (2011).
[30] Ojefors E., Grzyb J., Zhao Y., Heinemann B., Tillack B., and Pfeiffer U. R., "A 820GHz SiGe Chipset for Terahertz Active Imaging Applications," *IEEE International Solid-State Circuits Conference* (2011).
[31] "OpenFx," ,http://www.openfx.org/, Last accessed 20 Mar. 2012.